Subbarrier interactions of the oxygen isotopes

V. Pönisch* and S. E. Koonin
W. K. Kellogg Radiation Laboratory, California Institute of Technology, Pasadena, California 91125
(Received 30 March 1987)

We derive a unified description of the low-energy elastic, inelastic, neutron transfer, and fusion cross sections of systems involving two stable oxygen isotopes. Coupled channels equations with an incoming wave boundary condition are employed, as is the no-recoil approximation; the adiabatic approximation, which violates unitarity, is avoided. A calculation with phenomenologically determined $^{16}O + {}^{16}O$ and ^{16}O-n potentials reproduces the measured cross sections within the limitations of the model. A possible error in the data analysis for $^{16}O + {}^{17}O$ by Thomas *et al.* is pointed out.

I. INTRODUCTION

The description of subbarrier fusion in terms of a Schrödinger equation involving only the internuclear separation is quite adequate for many light systems. However, for heavier systems this picture often underpredicts experimental fusion cross sections below the barrier by large factors.[2] By "inverting" the measured fusion cross sections, Balantekin *et al.*[3] showed that this underprediction is due not to poor parametrization of the internuclear potential, but rather is inherent to a one-channel approach. A successful description of subbarrier fusion in these heavier systems is possible only if other degrees of freedom are treated explicitly; likely candidates include target and projectile excitations, as well as few-nucleon transfer.

Comparisons of closely related systems involving different isotopes or isotones of the target and/or the projectile allow an addition and removal of selected degrees of freedom and hence an isolation of their influence on the fusion process. The stable oxygen isotopes ^{16}O, ^{17}O, and ^{18}O are particularly attractive in this regard. The doubly magic ^{16}O nucleus has no low-energy excited states, the extra neutron in ^{17}O provides fairly clean single-particle states, and ^{18}O has well-defined two-neutron excitations. Moreover, in the $^{17,18}O + {}^{16}O$ systems, the one- or two-neutron transfer channels, respectively, have vanishing Q value and are thus expected to enhance the subbarrier fusion cross section. The coherent addition of this transfer amplitude in the elastic channel results in a rich structure in the angular distributions. There have been several measurements of the $^{16}O + {}^{16}O$ subbarrier fusion cross section,[1,4–7] and Thomas *et al.*[1,7] have measured $^{16}O + {}^{17}O$ and $^{16}O + {}^{18}O$. Data for various angular distributions are also available.[6,8–12]

In this paper we attempt a unified description of the subbarrier elastic, inelastic, transfer, and fusion cross sections for systems involving two oxygen isotopes. Our basic picture is two inert ^{16}O cores interacting with valence neutrons and with each other. Given a phenomenological, but microscopic, description of the low-lying states in ^{17}O and ^{18}O and of the $^{16}O + {}^{16}O$ system, we wish to assess the effects of the neutron degrees of freedom on the experimental observables of the $^{17}O + {}^{16}O$ and $^{18}O + {}^{16}O$ systems. Our computational framework is the coupled channels formalism, supplemented by an incoming wave boundary condition (IWBC). In Sec. II we define our model for the $^{17}O + {}^{16}O$ system and compare its predictions with the data. In Sec. III we similarly consider the $^{18}O + {}^{16}O$ system. Some conclusions are given in Sec. IV. Details of this work can be found in Ref. 13.

II. THE $^{16}O + {}^{17}O$ SYSTEM

We treat the $^{16}O + {}^{17}O$ system as a three-body problem of two inert ^{16}O cores interacting with each other and with a valence neutron. This allows us to account simply for the $\frac{5}{2}^+$ ground state and $\frac{1}{2}^+$ excited state of ^{17}O and for the exchange symmetry between the two ^{16}O cores. The dynamics are determined by the core-core potential V, and an ^{16}O-neutron potential, v. After eliminating the center-of-mass coordinates, we choose the intercore separation, $\mathbf{R}$, and the neutron center-of-mass location, $\mathbf{r}$, as independent coordinates, as shown in Fig. 1. The Hamiltonian is then

$$H = -\frac{\hbar^2}{M}\nabla_R^2 - \frac{\hbar^2}{2\mu}\nabla_r^2 + V(|\mathbf{R}|) + v(|\mathbf{r}+\tfrac{1}{2}\mathbf{R}|) + v(|\mathbf{r}-\tfrac{1}{2}\mathbf{R}|)\,, \quad (1)$$

where M is the ^{16}O mass (twice the reduced mass for the

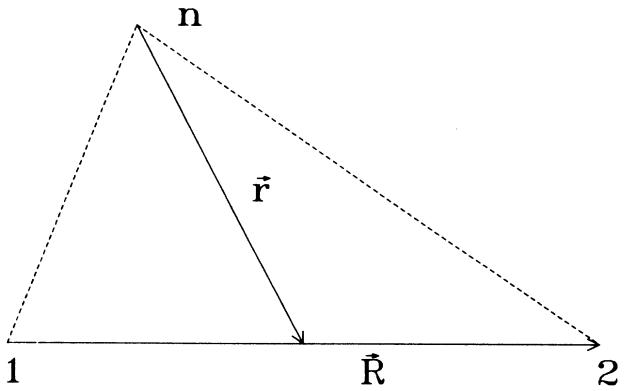

FIG. 1. Coordinates for the $^{17}O + {}^{16}O$ model; 1 and 2 refer to the two ^{16}O cores and n refers to the valence neutron.

$^{16}O + {}^{16}O$ system) and μ is the reduced mass for the (two ^{16}O)-n system; i.e., $\mu = 2Mm/(2M+m)$, with m the neutron mass. To complete the model, we use phenomenological considerations to specify the potentials involved.

A. The core-core potential

The $^{16}O + {}^{16}O$ fusion cross section is well reproduced in an IWBC framework by a one-channel Schrödinger equation involving a real internucleus potential. Writing V as the sum of a nuclear potential, V_N, and the Coulomb potential between two point $Z=8$ charges, Thomas *et al.* chose a Woods-Saxon form

$$V_N(R) = \frac{-V_0}{1+\exp[(R-R_0)/a]} \ . \tag{2}$$

They fixed the potential depth V_0 and performed a two-parameter least-squares fit to the fusion cross section by varying the potential radius R_0 and the diffuseness a. The quality of the fit is very insensitive to the choice of IWBC radius. Equally good fits were achieved with different values of V_0; they chose $V_0 = 50$ MeV and obtained $R_0 = 6.51$ fm and $a = 0.46$ fm. This same potential reproduces the 90° elastic differential cross section measured by Spinka and Winkler,[4] as well as the elastic angular distributions measured by Bromley *et al.*[6] and Wu and Barnes.[8]

The potential described above is very steep (i.e., a is very small), relative to typical folding potentials.[14] Nevertheless, it gives a good description of the $^{16}O + {}^{16}O$ system in a single-channel model. This is possible because the high excitation energy of the first excited state in ^{16}O(6.04 MeV) renders channel coupling small. This same rigidity encourages us to assume inert ^{16}O cores for the systems we treat and to adopt the potential of Thomas *et al.* for our model.

B. The core-neutron potential

The $J^\pi = \frac{5}{2}^+$ ground and $\frac{1}{2}^+$ (0.87 MeV) first excited states of ^{17}O are well described by single neutron $d_{5/2}$ and $s_{1/2}$ configurations, respectively. [Spectroscopic factors $S_{5/2} = 0.81$ and 0.78 have been measured in the $^{16}O(d,p)^{17}O$ reaction at a bombarding energy of $E_d = 25.4$ MeV, with a tendency for S to increase with increasing bombarding energy.[15]] A purely central ^{16}O-n potential with a realistic radial shape will reproduce neither the absolute binding nor relative splitting of these two single-particle orbitals, as the $1d$ orbital typically is less bound than the $2s$; the spin-orbit potential is essential. However, introduction of a spin-orbit component of the core-neutron potential would significantly increase the number of reaction channels that couple to each other and the overall complexity of our calculation. We have therefore chosen a central ^{16}O-n potential with a somewhat unconventional radial shape that places the $1d$ and $2s$ levels at the appropriate energies; the more deeply bound levels of this potential are ignored. We also ignore the experimental $\frac{1}{2}^-$ and $\frac{5}{2}^-$ states of ^{17}O; these are expected to be unimportant because of their high Q value and negative parity, as is confirmed in the data of Thomas *et al.*[1]

Our ^{16}O-n potential is the sum of Woods-Saxon and Gaussian terms:

$$v(r) = \frac{-v_0}{1+\exp[(r-r_0)/a]} + v_1 \exp(-r^2/r_1^2) \ , \tag{3}$$

with the parameters $v_0 = 60.827$ MeV, $v_1 = 27.3$ MeV, $r_0 = 3.034$ fm, $a = 0.66$ fm, and $r_1 = 1.0$ fm. Here, the Woods-Saxon term has the same diffuseness a and radius r_0 as the ^{17}O potential of Ref. 16. When inserted into the Schrödinger equation defining the single-particle orbitals,

$$\left[-\frac{\hbar^2}{2\bar{\mu}} \nabla_r^2 + v(\,|\,\mathbf{r} \pm \tfrac{1}{2}\mathbf{R}\,|\,) \right] \phi_i(\mathbf{r} \pm \tfrac{1}{2}\mathbf{R}) = \epsilon_i \phi_i(\mathbf{r} \pm \tfrac{1}{2}\mathbf{R}) \ , \tag{4}$$

where i labels the orbital being considered, ϵ_i is the single-particle energy, and $\bar{\mu} = Mm/(M+m)$ is the reduced mass of the ^{16}O-n system, the physically correct $1d$ and $2s$ eigenvalues are reproduced. We note that our procedure of fitting the eigenvalues of our potential to the experimental ^{17}O levels guarantees that the exponential falloff of the radial wave function is correct, although its normalization at large neutron-core separations depends upon the detailed form of v that we have chosen. Our potential produces asymptotic normalizations of 0.362 $\text{fm}^{-3/2}$ for the $d_{5/2}$ ground state and 1.172 $\text{fm}^{-3/2}$ for the $s_{1/2}$ state, while Gelbke *et al.*[9] give 0.363 and 1.133 $\text{fm}^{-3/2}$, respectively, and Burzynski *et al.*[10] give 0.354 $\text{fm}^{-3/2}$ for the $d_{5/2}$ state.

C. The coupled channels equations

Our *ansatz* for the total wave function $|\,\Phi\rangle$ is a sum over products of channel wave functions $\Phi_i(\mathbf{R})$ and internal single neutron states $|\,i\rangle$ in ^{17}O. We include in the latter only the $1d_{5/2}$ and $2s_{1/2}$ orbitals and use the letters α and β to denote the partition of the system; i.e., whether the neutron forms ^{17}O together with the "left" or "right" ^{16}O core. Thus,

$$|\,\Phi\rangle = \sum_i \Phi_{i\alpha}(\mathbf{R})\,|\,\alpha,i\rangle + \sum_j \Phi_{j\beta}(\mathbf{R})\,|\,\beta,j\rangle \ , \tag{5}$$

or, equivalently,

$$|\,\Phi\rangle = \sum_i \Phi_{i\alpha}(\mathbf{R})\phi_i(\mathbf{r}+\tfrac{1}{2}\mathbf{R}) + \sum_j \Phi_{j\alpha}(\mathbf{R})\phi_j(\mathbf{r}-\tfrac{1}{2}\mathbf{R}) \tag{6}$$

if the internal wave functions are written explicitly in coordinate space. The ϕ_i are, of course, spinors describing the neutron's spin.

The kinetic energy in the full Hamiltonian (1) associated with the neutron center-of-mass coordinate $\mathbf{r}$ contains the (two-^{16}O) + neutron reduced mass, μ, while the single-particle Schrödinger equation defining the neutron-core bound states involves the ^{16}O-n reduced mass, $\bar{\mu}$. Equating these two reduced masses is a particular no-recoil approximation, which becomes exact in the limit $m/M \to 0$. This step seems to us to be the cleanest way of treating the coupled channels problem with transfer as a system of local differential equations (an alternative is to

simulate the nonlocality of the exact equations by scaling[17]). However, we will show below that it allows the adiabatic approximation only at the cost of nonunitarity and that the alternative nonadiabatic coupled channels equations contain first-order derivatives.

The coupled channels equations are derived by projecting the Schrödinger equation with the kets $\langle k\alpha \mid$ and $\langle k\beta \mid$:

$$
\begin{aligned}
0&=\langle k\alpha \mid H-E \mid \Phi\rangle \\
&=\left[-\frac{\hbar^2}{M}\nabla_R^2-E+\epsilon_k+V(\mid \mathbf{R}\mid)\right]\Phi_{k\alpha}(\mathbf{R}) \\
&+\sum_i \Phi_{i\alpha}(\mathbf{R})\int d^3r\,\phi_k^*(\mathbf{r}+\tfrac{1}{2}\mathbf{R})\left[-\frac{\hbar^2}{M}\nabla_R^2+v(\mid \mathbf{r}-\tfrac{1}{2}\mathbf{R}\mid)\right]\phi_i(\mathbf{r}+\tfrac{1}{2}\mathbf{R}) \\
&+\sum_j \int d^3r\,\phi_k^*(\mathbf{r}+\tfrac{1}{2}\mathbf{R})\phi_j(\mathbf{r}-\tfrac{1}{2}\mathbf{R})\left[-\frac{\hbar^2}{M}\nabla_R^2-E+\epsilon_j+V(\mid \mathbf{R}\mid)\right]\Phi_{j\beta}(\mathbf{R}) \\
&-\frac{2\hbar^2}{M}\sum_j[\nabla_R\Phi_{j\beta}(\mathbf{R})]\cdot\left[\int d^3r\,\phi_k^*(\mathbf{r}+\tfrac{1}{2}\mathbf{R})\nabla_R\phi_j(\mathbf{r}-\tfrac{1}{2}\mathbf{R})\right] \\
&+\sum_j \Phi_{j\beta}(\mathbf{R})\int d^3r\,\phi_k^*(\mathbf{r}+\tfrac{1}{2}\mathbf{R})\left[-\frac{\hbar^2}{M}\nabla_R^2+v(\mid \mathbf{r}+\tfrac{1}{2}\mathbf{R}\mid)\right]\phi_j(\mathbf{r}-\tfrac{1}{2}\mathbf{R}) ,
\end{aligned}
\tag{7}
$$

and similarly for $\langle k\beta \mid$. Here, we have used the facts that

$$\int d^3r\,\phi_k^*(\mathbf{r}+\tfrac{1}{2}\mathbf{R})\nabla_R\phi_i(\mathbf{r}+\tfrac{1}{2}\mathbf{R})=0$$

(we consider only internal states of the same parity), and that

$$\int d^3r\,\phi_k^*(\mathbf{r}+\tfrac{1}{2}\mathbf{R})\nabla_R^2\phi_i(\mathbf{r}+\tfrac{1}{2}\mathbf{R})$$

is independent of $\mathbf{R}$ and is equal to $\delta_{ik}T_k/4$, where $T_k=\int d^3x\phi_k^*(\mathbf{x})\nabla_x^2\phi_k(\mathbf{x})$.

A considerable simplification and a halving in the number of channels that couple to each other can be achieved by working in an even/odd basis, rather than the left/right basis used above. We define even/odd state as

$$\mid i,p\rangle=2^{-1/2}[\mid i,\alpha\rangle+(-1)^p\mid i,\beta\rangle] , \tag{8}$$

where p takes the values 0 (even) and 1 (odd). The exchange symmetry of the two ^{16}O cores implies that matrix elements of the potential, overlap, and differential operators ∇_R and ∇_R^2 are diagonal in p. Thus, for each k, Eq. (7) and its analog for $\langle k,\beta \mid$ are transformed into uncoupled equations for the even and odd states; the coupling in the indices k, i, and j remains, however.

With the definitions and derived identities

$$
\begin{aligned}
\langle kp \mid ip\rangle&=\delta_{ik}+(-1)^p\langle k\alpha \mid i\beta\rangle \\
&=\delta_{ik}+(-1)^p\langle k\beta \mid i\alpha\rangle , \\
\langle kp \mid V_x \mid ip\rangle&=\langle k\alpha \mid V_- \mid i\alpha\rangle+(-1)^p\langle k\beta \mid V_- \mid i\alpha\rangle \\
&=\langle k\beta \mid V_+ \mid i\beta\rangle+(-1)^p\langle k\alpha \mid V_+ \mid i\beta\rangle ,
\end{aligned}
\tag{9}
$$

$$\langle k\alpha \mid \nabla \mid i\beta\rangle=\langle k\beta \mid \nabla \mid i\alpha\rangle ,$$

$$\langle k\alpha \mid \nabla^2 \mid i\beta\rangle=\langle k\beta \mid \nabla^2 \mid i\alpha\rangle ,$$

where V_+ and V_- are given in coordinate space by $v(\mid \mathbf{r}+\frac{1}{2}\mathbf{R}\mid)$ and $v(\mid \mathbf{r}-\frac{1}{2}\mathbf{R}\mid)$, respectively, the coupled channels equations can be written as

$$
\begin{aligned}
0=\sum_i\Bigg\{&\left[(-E+\epsilon_i+V)\langle kp \mid ip\rangle+\delta_{ik}T_k/4+\langle kp \mid V_x \mid ip\rangle-\frac{\hbar^2}{M}\langle k\alpha \mid \nabla^2 \mid i\beta\rangle\right]\Phi_{ip} \\
&-\frac{2\hbar^2}{M}\langle k\alpha \mid \nabla \mid i\beta\rangle\cdot(\nabla\Phi_{ip})-\frac{\hbar^2}{M}\langle kp \mid ip\rangle\nabla^2\Phi_{ip}\Bigg\}
\end{aligned}
\tag{10}
$$

for all k. Here, the even/odd channel wave functions are

$$\Phi_{ip}(\mathbf{R})=\Phi_{i\alpha}(\mathbf{R})+(-1)^p\Phi_{i\beta}(\mathbf{R}) , \tag{11}$$

and the core-core potential V and all matrix elements in Eq. (9) are functions of $\mathbf{R}$.

The no-recoil approximation and the resulting constant T_i in Eq. (10) lead to an ambiguity in the Q value. On the one hand, it can be defined as the difference in kinetic energy at spatial infinity for different channels; alternatively, it is the difference of the single-particle energies in ^{17}O. In an exact calculation, these are, of course, equivalent. We have used the former definition in our numerical calculations to guarantee the correct asymptotic behavior of the channel wave functions and thus treat the

dynamical effects of the Q values correctly.

Using the rotational symmetries of the problem and angular momentum couplings, Eq. (10) can be transformed into a set of differential equations for radial wave functions involving only $R = |\mathbf{R}|$ and the matrix elements can be reduced from three- to two-dimensional integrals that can be evaluated by numerical quadrature. The appearance of first-order derivatives in Eq. (10) prohibits use of the usual Numerov algorithm[18] for discretization. Thus, we have employed a simpler formula that is of second order in the step size. The usual method for coupled channels Schrödinger equations, namely the sequential Born-series-like channel-by-channel integration,[19] then loses much of its advantage over a direct calculation where all channels are integrated outwards simultaneously. This is especially true for systems with few coupled channels. In the even/odd basis we have for the general case four channels that have the same parity: the three ground state channels with total channel spin $J=\frac{5}{2}$ and the one excited state channel with $J=\frac{1}{2}$.

D. IWBC for coupled channels

The IWBC is formulated for the multichannel case as

$$\chi_{ip}(R)\sim[\kappa_{ip}(R)]^{-1/2}\exp\left[-i\int_{R_0}^{R}\kappa_{ip}(\bar{R})d\bar{R}\right] \quad (12)$$

for R near R_0, where R_0 is the IWBC radius and

$$\kappa_{ip}=\left[\frac{2\bar{M}E_{ip}}{\hbar^2\langle ip\,|\,ip\rangle}\right]^{1/2}, \quad (13)$$

with $\bar{M}$ the reduced mass of ^{16}O-^{17}O, and E_{ip} the energy of channel (i,p) at $R=\infty$.

The set of equations (10) is unusual in direct reaction theory studies because it contains first-order derivatives of the channel function Φ_{ip}. An approximation that eliminates these terms is to let ∇_R^2 in Eq. (1) act only on the $\mathbf{R}$ dependence of $\Phi_{i\alpha/\beta}$ in Eqs. (5) and (6), but not on the internal wave function ϕ_i. We call this the adiabatic (or Born-Oppenheimer) approximation in analogy to molecular physics, because the potential of the light particle (here the neutron) is calculated with the positions of the heavy particles (here the ^{16}O cores) fixed. This calculation, however, is done only on the truncated subspace of ^{17}O wave functions for either core.

The existence of a conserved probability current for the coupled channels equations we use is very desirable since far below the barrier it is much easier to evaluate the fusion cross section by calculating the in-going flux at the IWBC radius, rather than from the small outgoing flux missing at large separations. Unfortunately, the coupled channels equations resulting from the adiabatic approximation do not admit a conserved current. The flux in the nonorthogonal basis states is

$$\mathbf{F}=\frac{\hbar}{2\bar{M}i}\sum_{\gamma=\alpha}^{\beta}\sum_{\delta=\alpha}^{\beta}\sum_{i,j}\langle i\gamma\,|\,j\delta\rangle(\Phi_{i\gamma}^{*}\nabla\Phi_{j\delta}-\Phi_{j\delta}\nabla\Phi_{i\gamma}^{*}) . \quad (14)$$

It is easy to show that $\mathbf{F}$ is conserved by Eq. (10), but not in the adiabatic approximation. (Approximate, but nontrivial expressions for $\mathbf{F}$ are also not conserved in the latter.) The loss of unitarity in the IWBC framework makes the definition of the fusion cross section ambiguous because the difference in flux of the incoming and total outgoing wave is not equal to the flux at the IWBC radius. Therefore, we have not made the adiabatic approximation in our work and have returned the first derivatives in Eq. (10).

E. Results and comparison with experiment

Figure 2 shows our calculated fusion excitation function and the corresponding experimental data. Two data sets are shown: the open circles are the data published by Thomas *et al.*,[1] while the error bars are the same data corrected for an error in the determination of the ^{28}Al partial fusion cross section.[20] The new cross section data show a small, but clearly visible, enhancement over the ^{16}O + ^{16}O fusion cross section (dashed line in Fig. 2), which is well reproduced by our calculation (solid line in Fig. 2).

Figure 3 shows the total inelastic excitation function for ^{16}O + ^{17}O$\rightarrow$^{16}O + ^{17}O$^{*}_{1/2}$. The data are from Ref. 1, the solid line is our calculation, and the dashed line is a semiclassical Coulomb excitation calculation.[21] At these energies, the Coulomb excitation cross section is very small compared to the nuclear excitation and thus has a negligible effect on the fusion process. The large inelastic cross section at low energy stems not from the direct inelastic reaction, but from neutron transfer into the excited state. In the no-recoil approximation, this transfer is not affected by the Coulomb force. The experimental cross section is consistently smaller than the calculated one, from a factor 0.25 at the lowest to 0.7 at the above-barrier energies. This could, of course, be improved at the expense of fitting the parameters in our calculation (e.g., the neutron-core potential).

Figure 4 shows an experimental inelastic angular distribution from Ref. 9 and our calculation (dashed line). The interference pattern in the cross section stems from the

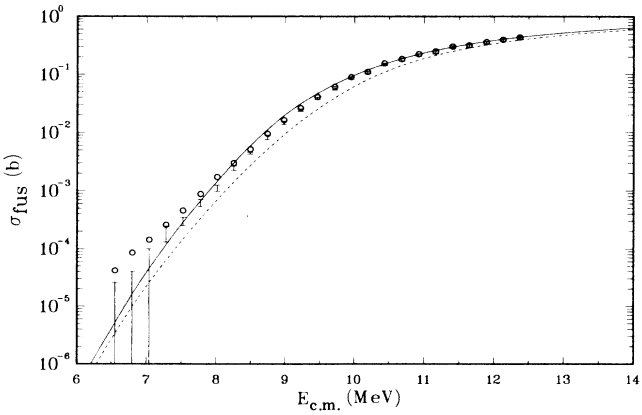

FIG. 2. Fusion cross section for ^{17}O + ^{16}O. The circles depict the data from Ref. 1. The error bars are centered around the corrected values, as discussed in the text, but their sizes are unchanged. The solid line is the result of our calculation, while the dashed line shows the calculated ^{16}O + ^{16}O fusion cross section.

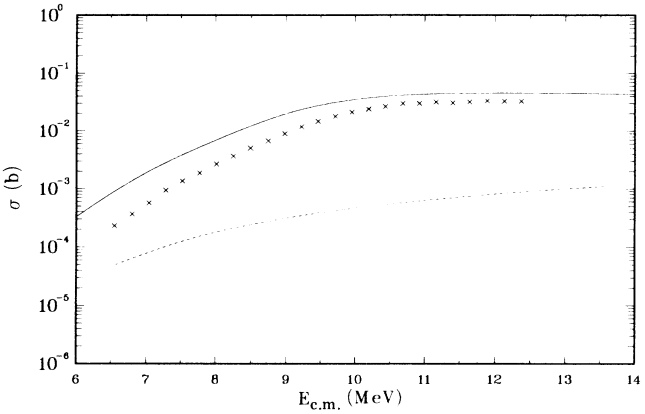

FIG. 3. Total inelastic cross section $^{17}O + {}^{16}O \rightarrow {}^{17}O^* + {}^{16}O$. The crosses are the data from Ref. 1 (errors are smaller than the symbol size). The lines show the result of the calculated nuclear (solid) and Coulomb excitation cross sections (dashed).

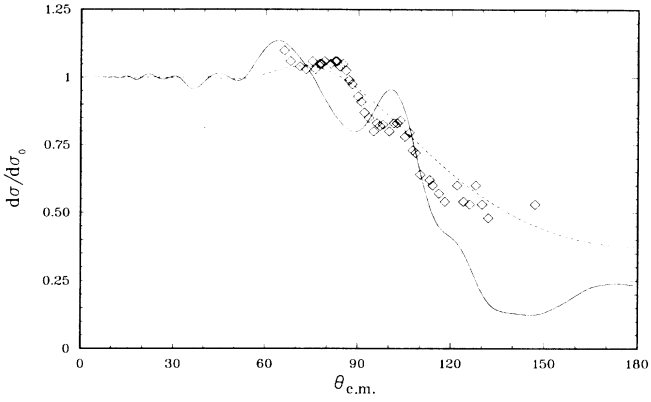

FIG. 5. Ratio of the elastic cross section, $d\sigma/d\Omega$, to the Rutherford cross section, $d\sigma_0/d\Omega$, for $^{17}O + {}^{16}O$ at $E_{c.m.} = 10.67$ MeV; data are from Ref. 10. The solid line results from our coupled channels calculation, while the dashed line is a one-channel calculation using the ^{16}O-^{16}O potential.

coherent summing of the direct inelastic and transfer elastic amplitudes. The solid line is the result of our calculation scaled by a factor 0.7, i.e., the factor that would bring the total measured and calculated cross sections into agreement at these energies. After scaling, the data are fairly well reproduced (of the same quality as the DWBA calculation of Ref. 9, which needed a scaling factor of the same magnitude).

The elastic angular distribution relative to the Rutherford cross section at $E_{c.m.} = 10.65$ MeV is shown in Fig. 5. The measurements are from Burzynski *et al.*[10] and the solid curve is our result. The dashed curve is a one-channel calculation that uses just the ^{16}O-^{16}O potential without transfer or inelastic excitation. The data exhibit oscillatory behavior around this curve; again, this is due to the interference of the direct elastic and transfer elastic channel. Burzynski *et al.* find an excellent fit to these oscillations with an exact finite-range distorted-wave Born-approximation calculation with a fitted spectroscopic factor, i.e., a scaling of their single-particle wave function

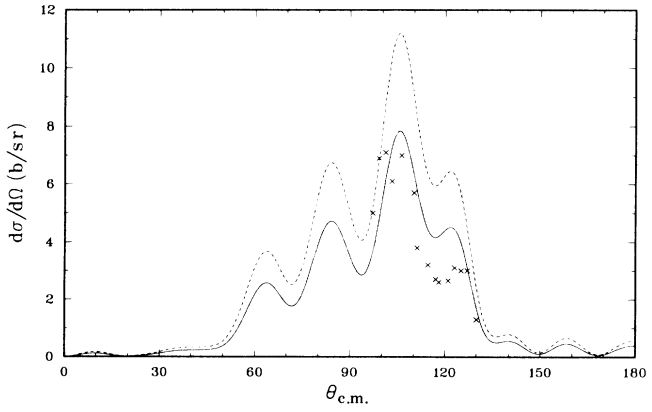

FIG. 4. Inelastic differential cross section for $^{17}O + {}^{16}O$ at $E_{c.m.} = 11.3$ MeV. The data are from Ref. 9 and the solid and dashed lines show our scaled and unscaled results, respectively.

and thus matrix elements. Also, their single-particle potential contains a spin-orbit coupling term. Our full calculation (solid curve) shows the same oscillations, but they are too pronounced at larger angles. We might attribute this deviation either to a relatively poor choice of the single-particle wave function (e.g., an absence of a spin-orbit coupling term in the single-particle potential) and/or to our no-recoil approximation.

III. THE $^{16}O+{}^{18}O$ SYSTEM

We model the ^{16}O-^{18}O system at subbarrier energies in the same spirit as the ^{16}O-^{17}O calculation described above. The ^{16}O-^{16}O potential is taken from Thomas *et al.* and the coupling matrix elements are derived from the single-particle potential (3). However, because of the higher excitation energy of the first excited state in ^{18}O (1.98 MeV, compared to 0.87 MeV in ^{17}O), the total inelastic (direct and transfer) cross section for ^{18}O-^{16}O is much lower than that for ^{17}O-^{16}O. (Figures 6 and 3 show the measurements for these two systems.) A semiclassical Coulomb excitation calculation of the first excited state (no other excitations were observed in the experiments) shows that Coulomb excitation accounts for all of the inelastic cross section below $E_{c.m.} = 10$ MeV (solid line in Fig. 6). We conclude that the inelastic channels are unimportant for the subbarrier fusion process but that, should they be taken into account, nuclear excitation (as in our treatment of the ^{16}O-^{17}O system) must be supplemented by Coulomb excitation. We therefore do not include inelastic channels in our description of the fusion cross section and restrict our calculation to only the direct and two-neutron transfer elastic channels.

Our model is the three-body system of two ^{16}O cores and one effective dineutron "boson." The same no-recoil approximation is made and the same formalism is used as in Sec. II B (again, the final equation contains a first derivative of the channel wave function). The neutron-neutron interaction is treated as a perturbation to first or-

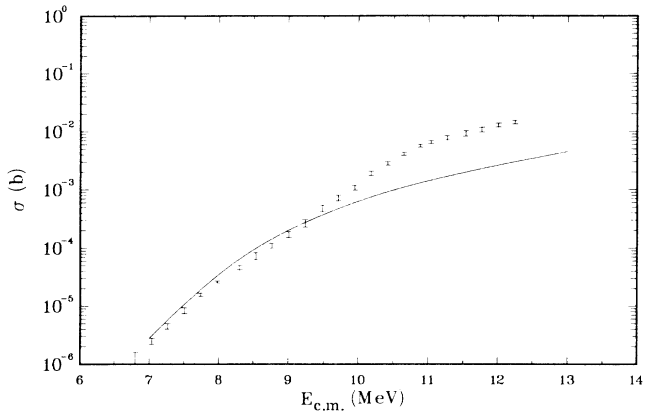

FIG. 6. Total inelastic cross section $^{18}O + {}^{16}O \rightarrow {}^{18}O^* + {}^{16}O$. Data are from Ref. 1 and the solid line shows the result of a Coulomb excitation calculation.

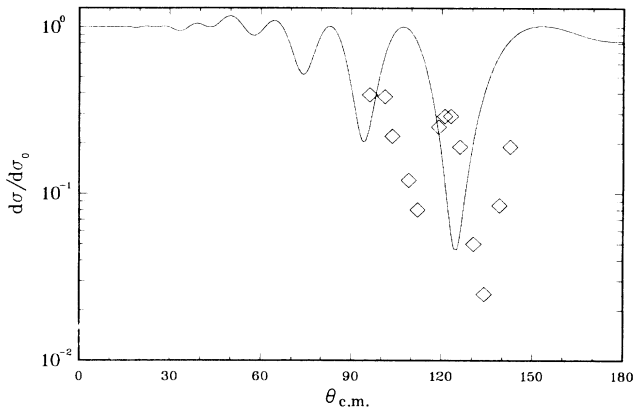

FIG. 8. Ratio of elastic cross section $d\sigma/d\Omega$ to Rutherford cross section $d\sigma_0/d\Omega$, for $^{18}O + {}^{16}O$ at $E_{c.m.} = 12.7$ MeV; data are from Ref. 11.

der in the energy and to zeroth order in the wave functions; i.e., ^{17}O radial wave functions are used with the correct angular momentum coupling. In an even/odd basis the coupled channels system is reduced to two uncoupled single-channel equations. Details of the calculation can be found in Ref. 13.

We show our calculated fusion cross section (solid line) in Fig. 7 together with the data from Refs. 1 and 7 and the ^{16}O-^{16}O results (dashed line) for comparison. The subbarrier fusion enhancement is well reproduced. Above the barrier (~ 10 MeV) the measured fusion cross section exhibits a dip that the calculation does not reproduce. If this structure is real, it could arise from the interference of the direct channel with another channel. Our calculation makes it unlikely that this would be the transfer elastic channel, and the small inelastic cross section makes it unlikely that excited states are involved. We conclude that this above-barrier structure remains unexplained.

Because of the simplicity of our ^{18}O wave function, we cannot expect that the elastic angular distributions are reproduced any better than are those for $^{16}O + {}^{17}O$.

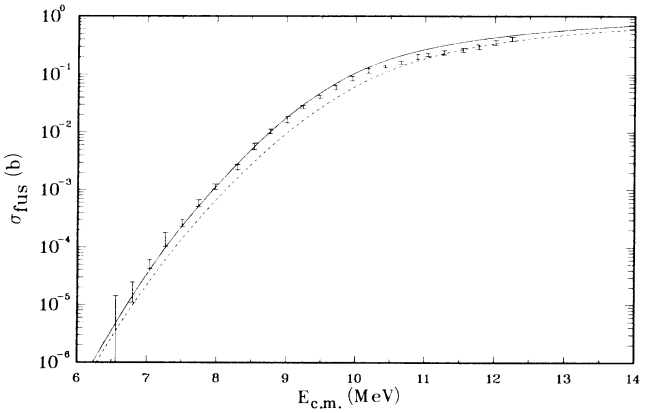

FIG. 7. Fusion cross section for $^{18}O + {}^{16}O$; data are from Ref. 1. The solid line is the result of our calculation, while the dashed line shows the calculated $^{16}O + {}^{16}O$ fusion cross section.

Indeed, Fig. 8 shows only qualitative agreement between the calculation and the measurement by Gelbke *et al.*[11]

IV. CONCLUSION

The subbarrier fusion cross sections for $^{17}O + {}^{16}O$ and $^{18}O + {}^{16}O$ show relatively little enhancement over that for $^{16}O + {}^{16}O$ when compared with isotope differences for heavier systems. These enhancements are well reproduced in our model calculation, with the possible exception of an above-barrier structure apparent in the $^{16}O + {}^{18}O$ data of Refs. 1 and 7. Our consistent incorporation of inelastic and transfer channels allowed us to calculate various differential cross sections as well. In all cases considered, our results show qualitative agreement with experiment.

An improved quantitative agreement with much of the experimental data could no doubt be had by a fine tuning of the single-particle potential and wave functions. In our model calculations, the quality of the single-particle wave functions sets a limit on how realistic is our description of the additional channels in the fusion system and hence how believable are our precise values of the fusion cross section. We did not perform such a fit in this work, but believe that we have demonstrated the feasibility of doing so. A truly unified picture of all aspects of collisions at subbarrier energies (to the formation of the compound nucleus) has been obtained in this way.

For internal consistency in models that include particle transfer (and hence nonorthogonal basis states) it is necessary to avoid the adiabatic approximation, if a no-recoil approximation is made and only ordinary differential equations are to be solved. However, the nonadiabatic equations contain first-order derivatives and are more difficult to integrate numerically.

The remaining systems of oxygen isotopes amenable to experimental study pose interesting experimental and theoretical problems. From a theoretical point of view the $^{17}O + {}^{17}O$ system is especially interesting because of the positive Q value of the ^{16}O-^{18}O channel and the expected larger enhancement of the subbarrier fusion cross section.

ACKNOWLEDGMENTS

The authors thank C. A. Barnes, K. Langanke, and S.-C. Wu for helpful discussions, and especially A. Winther for his constructive criticism and many suggestions. Special thanks go to J. Thomas for pointing out his doubts about the data analysis of Ref. 1 and allowing us to include his suggestions in this paper. Financial support for this work has been provided by the National Science Foundation under Grants PHY83-07732, PHY85-05682, and PHY86-04197.

---

*Present address: Niels-Bohr-Institute, Blegdamsvej 17, DK-2100 Copenhagen Ø, Denmark.

[1]J. Thomas, Y. T. Chen, S. Hinds, D. Meredith, and M. Olson, Phys. Rev. C **33**, 1679 (1986).

[2]For a general overview, see *Fusion Reactions Below the Coulomb Barrier,* Vol. 219 of *Lecture Notes in Physics,* edited by S. Steadman (Springer, New York, 1985).

[3]A. B. Balantekin, S. E. Koonin, and J. W. Negele, Phys. Rev. C **28**, 1565 (1983).

[4]H. Spinka and H. Winkler, Nucl. Phys. **A233**, 456 (1974).

[5]G. Hulke, C. Rolfs, and H. P. Trautvetter, Z. Phys. A **297**, 161 (1980).

[6]S.-C. Wu and C. A. Barnes, Nucl. Phys. **A422**, 373 (1984).

[7]J. Thomas *et al.*, Phys. Rev. C **31**, 1980 (1985).

[8]D. A. Bromley, J. A. Kuehner, and E. Almqvist, Phys. Rev. **123**, 878 (1961).

[9]C. K. Gelbke *et al.*, Nucl. Phys. **A219**, 253 (1974).

[10]S. Burzynski *et al.*, Nucl. Phys. **A399**, 230 (1983).

[11]C. K. Gelbke *et al.*, Phys. Rev. Lett. **29**, 1683 (1972).

[12]For more references, see F. Ajzenberg-Selove, Nucl. Phys. **A375**, 1 (1982); **A460**, 1 (1986); **A392**, 1 (1983).

[13]V. Pönisch, Ph.D. thesis, California Institute of Technology, 1986 (available from University Microfilms Inc., Ann Arbor, MI).

[14]R. A. Broglia and A. Winther, *Heavy Ion Reactions Lecture Notes* (Benjamin-Cummings, Reading, MA, 1981), Vol. I, Chap. III.

[15]M. D. Cooper, W. F. Hornyak, and P. G. Roos, Nucl. Phys. **A218**, 249 (1974).

[16]G. Pollarolo, R. A. Broglia, and A. Winther, Nucl. Phys. **A406**, 369 (1983).

[17]R. A. Broglia *et al.*, Phys. Rep. **29**, 291 (1977).

[18]See, for example, S. E. Koonin, *Computational Physics* (Benjamin/Cummings, Menlo Park, CA, 1986), Chap. 3.

[19]M. Rhoades-Brown, M. H. MacFarlane, and S. C. Pieper, Phys. Rev. C **21**, 2417 (1980).

[20]In the original analysis of Ref. 1, the observed intensities of the 980 and 1017 keV lines of ^{28}Al were averaged to give the partial cross section. However, the 1017 keV line could have been confused with the 1014 keV line from ^{27}Al produced by a carbon contamination via $^{12}C + {}^{17}O \rightarrow {}^{27}Al + d$ (or even through $^{16}O + {}^{17}O \rightarrow {}^{27}Al + d + \alpha$). The new analysis uses only the intensity of the ^{28}Al 980 keV line (J. Thomas, private communication).

[21]K. Alder *et al.*, Rev. Mod. Phys. **28**, 432 (1956).